JACS
JOURNAL OF THE AMERICAN CHEMICAL SOCIETY
pubs.acs.org/JACS
Article

Solar-Driven Upcycling of Polystyrene Enabled by Elemental Sulfur

Yong Liu, Heng Liu,* Zhi-Hui Wang, Yilitabaier Julaiti, Zhang-Pei Chen,* Jian-She Hu,* and Qing-An Chen*

Cite This: J. Am. Chem. Soc. 2026, 148, 10193−10204
Read Online
ACCESS | Metrics & More | Article Recommendations | Supporting Information

ABSTRACT: Polystyrene (PS) is one of the most widely used plastics, and its notably low recycling rate has prompted the consideration of chemical upcycling of waste PS. Oxidative methodologies have been extensively investigated, employing molecular oxygen to upcycle PS into oxygenated products. Sulfur, a group congener of oxygen, has rarely been exploited in PS upcycling. Furthermore, elemental sulfur currently confronts an issue of an annual production surplus. Here, we report the coupcycling of PS and elemental sulfur into 2,4-diphenylthiophene and 1,3,5-triphenylbenzene by leveraging solar energy as the driving force. The practicality of this strategy is demonstrated by the rapid and efficient conversion of various postconsumer waste PS plastics under solvent-free, ambient air conditions. The photothermal effect of elemental sulfur and the generation of sulfur radicals at elevated temperatures are critical to enable this transformation. Experimental and computational studies of dimeric and tetrameric PS model compounds show that sulfur-radical-mediated hydrogen atom abstraction is the key to sustaining the reaction. These findings provide valuable insights into the photothermal behavior and reaction characteristics of elemental sulfur and hold significant implications for polymer conversion.

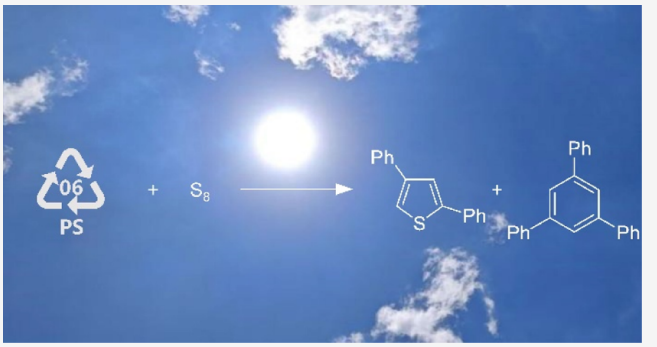

INTRODUCTION

Polystyrene (PS) ranks among the most widely used plastics, celebrated for its low cost, high durability, and broad applicability in food packaging, electrical appliances, automotive components, and more.[1] Globally, over 20 million tons of PS are produced annually, accounting for approximately 6% of the global plastic production (Figure 1a).[2] However, this material faces critical environmental challenges: its recycling rate remains extremely low (<1%), and it resists natural degradation in the environment.[3] The chemical inertness of PS stems from its molecular structure, where all atoms are linked by strong C−C (BDE of Csp^3−Csp^3: ∼77 kcal/mol) and C−H (BDE of Csp^3-H: ∼85 kcal/mol) covalent bonds (Figure 1b).[4] Thermochemical conversion methods, such as pyrolysis and hydrogenolysis, typically require substantial energy input to reach reaction temperatures (typically >300 °C).[5]

The conversion of PS under mild conditions has long been a research focus. Oxygen-mediated oxidative upcycling of PS stands out as a representative approach (Figure 1c). Composed of the group VIA element oxygen, the O_2 molecule features two unpaired electrons in its π^*2p molecular orbitals, functioning as a diradical that readily reacts with PS. Upon oxygenation, PS-derived oxygenated species can undergo β-scission to yield benzoic acid,[6] benzaldehyde,[7] benzoyl chloride,[7] acetophenone,[8] and benzamide[9] or proceed through the Hock rearrangement to form phenol and its derivatives.[4b,10]

The element sulfur, belonging to the same group as oxygen in the periodic table, whose elemental form (S_8) is a byproduct removed from crude oil and natural gas during petrochemical refining processes, is inexpensive and abundantly available.[11] With an annual production of 70 million tons, S_8 faces limited demand from existing applications, leading to millions of tons of S_8 being stored in open-air facilities for decades.[12] Notably, sulfur possesses a unique electronic structure, characterized by the high polarizability of lone-pair electrons in its 3p orbital and versatile redox capabilities across the oxidation state range from −2 to +6. This intrinsic feature endows sulfur-based dynamic covalent bonds with diverse responsive mechanisms, including redox, photolytic, and hydrolytic behavior.[13] Leveraging these properties, sulfur acts as a versatile building block for the fabrication of sulfur-containing degradable polymers. Inverse vulcanization represents a well-established synthetic strategy for such polymers, which proceeds via the generation of sulfur radicals from elemental sulfur and subsequent cross-linking with alkenes.[12,14] Elemental sulfur exists primarily in the form of an eight-membered ring under

Received: January 19, 2026
Revised: February 11, 2026
Accepted: February 17, 2026
Published: February 24, 2026

https://doi.org/10.1021/jacs.6c01318
J. Am. Chem. Soc. 2026, 148, 10193−10204

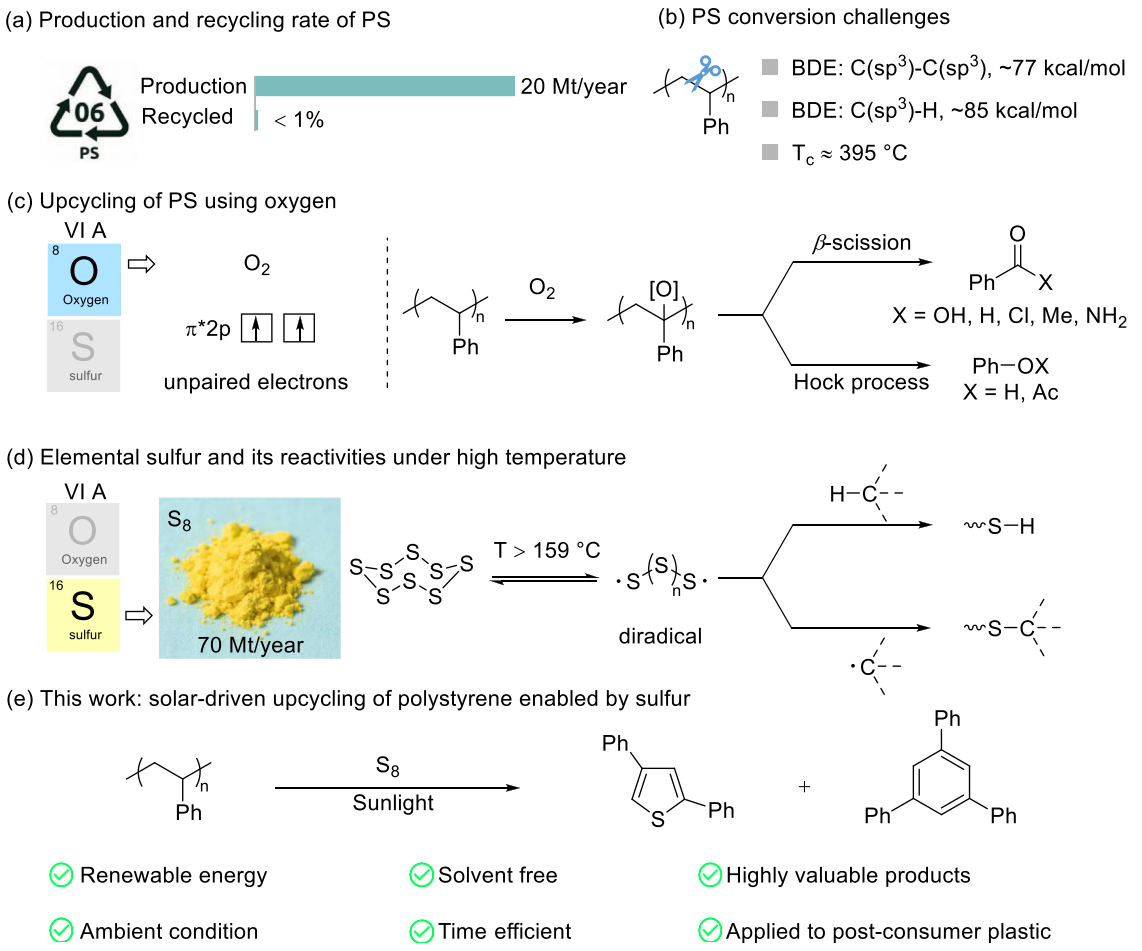

Figure 1. Upcycling of polystyrene using group VI A elements. (a) Production and recycling rate of PS. (b) PS conversion challenges. (c) Upcycling of PS using oxygen. (d) Elemental sulfur and its reactivities under high temperature. (e) This work: solar-driven upcycling of polystyrene enabled by sulfur.

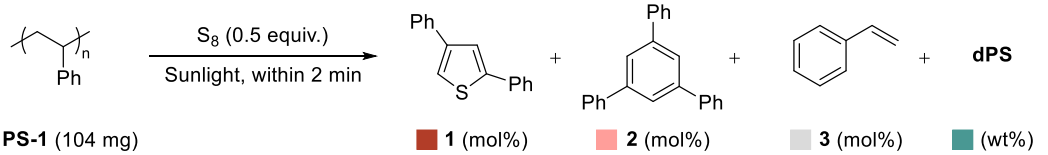

Entry	Variation from the standard conditions
1	none
2	w/o S_8
3	100 W LED instead of sunlight
4	ZnO was added
5	BaO was added
6	CB was added
7	Na_2S instead of S_8
8	Na_2SO_3 instead of S_8
9	Na_2SO_4 instead of S_8

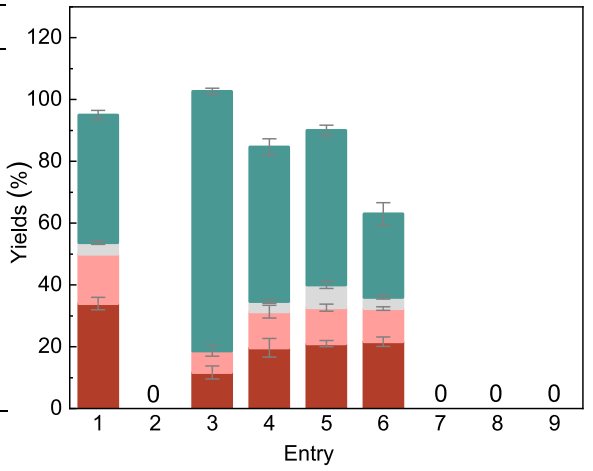

Figure 2. Optimization of the reaction conditions. The error bars represent the standard deviation of yield in 3 parallel experiments.

ambient conditions; yet above 159 °C, this cyclic structure undergoes ring-opening polymerization to yield linear polysulfanes with diradical chain ends.[14,15] These radical species demonstrate high reactivity, capable of both hydrogen

https://doi.org/10.1021/jacs.6c01318
J. Am. Chem. Soc. 2026, 148, 10193−10204

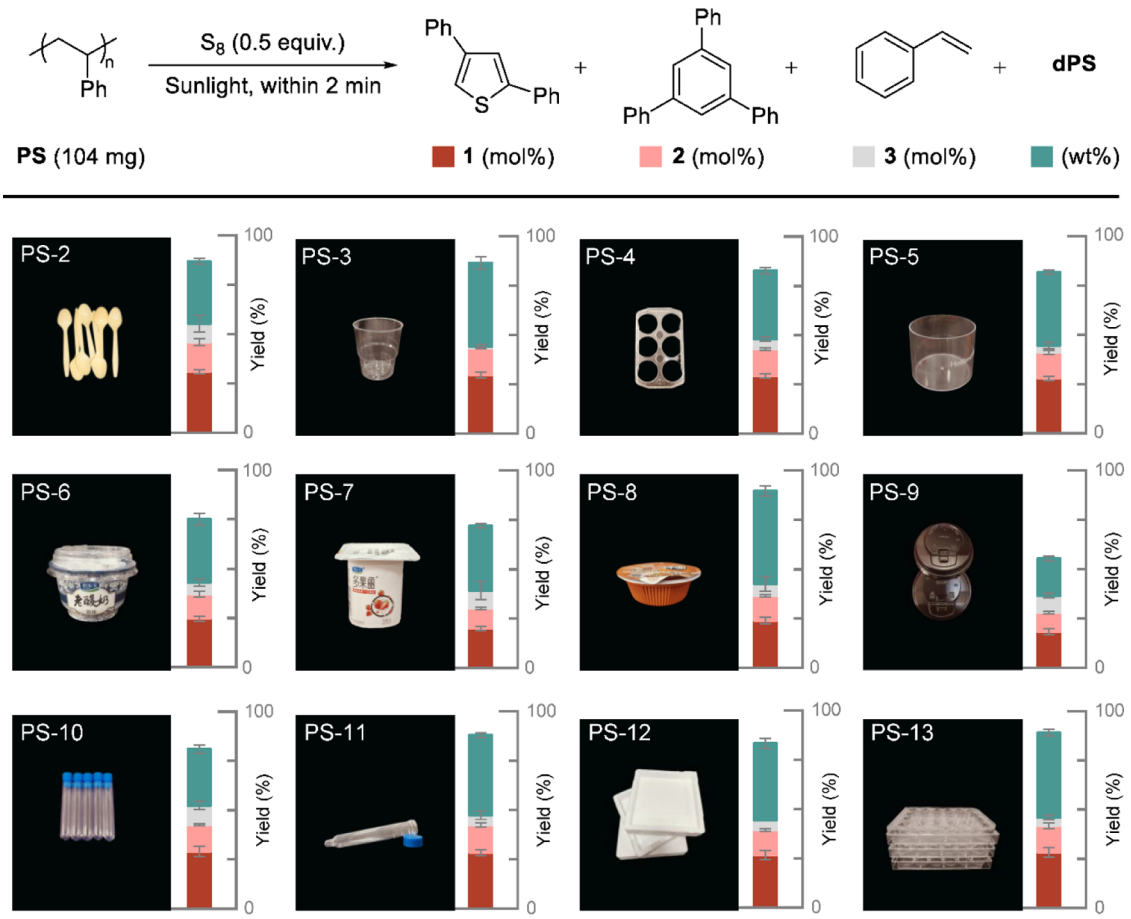

Figure 3. Upcycling of postconsumer waste PS plastics. The error bars represent the standard deviation of yield in 3 parallel experiments.

abstraction and carbon-radical coupling to form C−S bonds (Figure 1d).[16] These reactivities of elemental sulfur provide a feasible pathway for the coconversion of S_8 and plastics. This has been demonstrated by the use of sulfur to transform waste plastics into value-added carbon materials.[17] However, such conversions typically require high temperatures to ensure the generation of sulfur radicals, which consume substantial amounts of energy. Light offers a less energy-intensive approach for chemical recycling as well as unique selectivity and reactivity.[18] Light can excite photocatalysts to generate radicals, enabling plastic degradation under mild conditions.[19] It can also be converted to thermal energy to drive the plastic degradation process. Through photothermal conversion, the recycling of various plastics has been successfully achieved.[20] However, the coupcycling of PS and S_8 under photothermal conditions has not been fully explored.

Herein, we report a solar-driven coupcycling strategy for PS and S_8, yielding 2,4-diphenylthiophene and 1,3,5-triphenylbenzene (Figure 1e). This solvent-free reaction proceeds efficiently under ambient air conditions with high temporal efficiency, enabling the upcycling of various postconsumer plastic wastes. Mechanistic studies reveal that elemental sulfur serves dual roles as both a reactant and the initial photothermal agent, facilitating solar energy conversion and PS transformation. Reactions of dimeric and tetrameric PS model compounds with sulfur provide deep insights into the transformation mechanism of PS. Hydrogen atom abstraction (HAA) by sulfur radicals is identified as the key step for the coconversion of PS and S_8. The photothermal reactions of sulfur and the transformation mechanism of PS in this study will contribute to the advancement of sulfur chemistry and plastic upcycling.

RESULTS AND DISCUSSION

In contrast to previous studies,[20] where exogenous photothermal agents are required for the photothermal degradation of PS, our study commenced directly with the reaction of commercially available PS (**PS-1**, M_w: 396.9 kDa; M_n: 182.5 kDa) and S_8 (Figure 2). Following a careful screening of reaction conditions, a 40 cm diameter concave mirror was employed to focus sunlight (natural solar irradiance: 104 mW cm^{-2}, focal spot diameter: ∼4 cm) onto the mixture of PS and S_8 (Figure S1). Initially, partial melting of the reactants occurred alongside a gradual darkening of the color, after which the reaction proceeded rapidly. It was terminated upon complete conversion of the reactants to a reddish-black liquid, with the entire process concluding within 2 min. Upon completion, the reaction of 104 mg PS (1.0 mmol repeating units) with 0.5 equiv S_8 (4.0 mmol S atoms) afforded 2,4-diphenylthiophene (**1**) in 34% yield, 1,3,5-triphenylbenzene (**2**) in 16% yield, and a small amount of styrene (**3**) (entry 1). Additionally, partially degraded polystyrene (**dPS**, 41 wt % relative to PS) was isolated. Control experiments showed that target products were absent in the absence of S_8 (entry 2). Using an LED light source significantly reduced the product yields, leaving substantial amounts of **dPS** in the system (entry 3). However, the product yields could be improved by optimizing the reaction conditions (Tables S3−S5). Metal

https://doi.org/10.1021/jacs.6c01318
J. Am. Chem. Soc. 2026, 148, 10193−10204

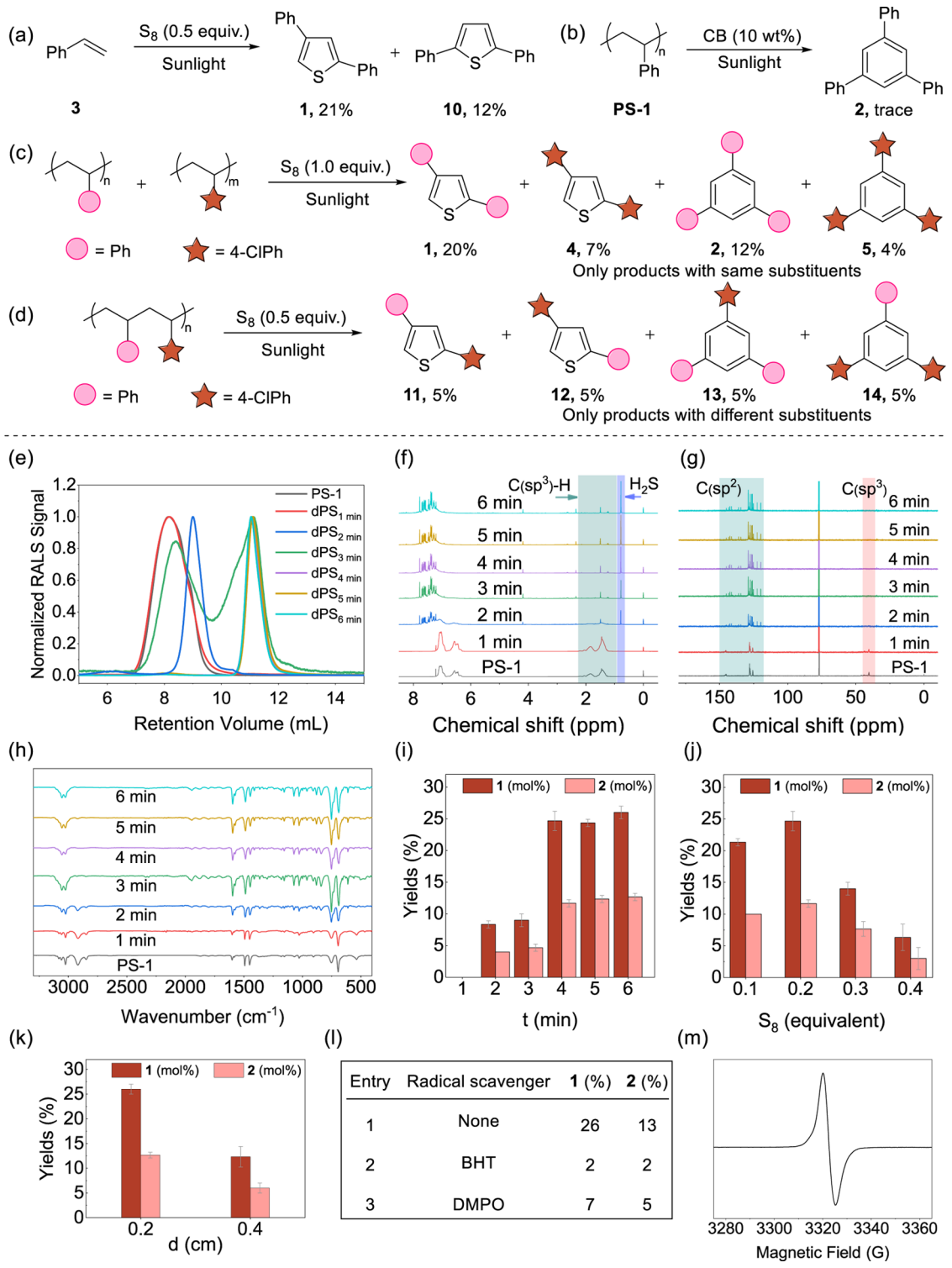

Figure 4. Mechanistic studies. (a) Reaction of styrene and S_8 under sunlight. (b) Conversion of PS under sunlight with CB (carbon black) as the photothermal agent. (c) Reaction of polymers with different monomers and S_8. (d) Conversion of alternating copolymer with S_8. (e) GPC analysis of **dPS** at different reaction times under white LED irradiation. (f) ^{1}H NMR spectra of the reaction at different reaction times under white LED irradiation. (g) ^{13}C NMR spectra of the reaction at different reaction times under white LED irradiation. (h) FT-IR spectra of the reaction at different reaction times under white LED irradiation. (i) Product yields at different reaction times under white LED irradiation. (j) Product yields with different S_8 dosages under white LED irradiation. (k) Product yields at different distances between the white LED and the reactor. (l) Radical scavenger experiments. (m) EPR spectroscopy of the mixture of PS and S_8 under white LED irradiation for 6 min.

oxides (ZnO and BaO) that can promote PS depolymerization[20b,21] both suppressed target product formation (entries 4 and 5). The addition of the extra photothermal agent (CB: carbon black) decreased target product **1** and **2** yields to 22% and 11%, respectively, and led to a significant increase in char formation (entry 6). This may arise from the photothermal agent accelerating PS chain scission and dehydrogenative carbonization. Compounds with other valent sulfur, Na_2S,

https://doi.org/10.1021/jacs.6c01318
J. Am. Chem. Soc. 2026, 148, 10193−10204

Na_2SO_3, and Na_2SO_4, all failed to convert PS to target products under sunlight irradiation (entries 7−9).

To elucidate the structure of **dPS** (Figure 2, entry 1), structural characterizations were conducted. The ^1H NMR spectrum of **dPS** exhibited negligible $C(sp^3)$-H signals (Figure S16), whereas its ^{13}C NMR spectrum displayed altered $C(sp^3)$ signals and new $C(sp^2)$ peaks (Figure S17). These spectral features revealed that **dPS** retained the aryl framework of pristine PS but underwent hydrogen elimination/substitution on saturated aliphatic chains. Gel permeation chromatography (GPC) confirmed a marked decrease in the molecular weight of **dPS** relative to the starting PS (Figure S5). Elemental analysis (EA) verified sulfur/oxygen incorporation in **dPS** (Table S9), while Fourier transform infrared (FT-IR) spectroscopy detected peaks at 1720 cm^{-1} (C═O stretching) and 1240 cm^{-1} (ketone skeletal vibration) (Figure S4). Although oxygen could be incorporated into the polymer chains, O_2 exerted no discernible effect on this reaction (Table S17). The characterization results demonstrate that **dPS** is a PS-derived product formed via partial chain scission coupled with the substitution and elimination of hydrogen atoms by sulfur and oxygen on the saturated aliphatic chains. Based on elemental analysis and spectroscopic characterization, we propose a plausible structural model for **dPS** (Figure S18), which may contain functional groups such as C═C, C−S/C═S, and minor C═O moieties formed via dehydrogenation and sulfur incorporation. The formation of these conjugated structures aligns with their significant photothermal activity.

With the optimal reaction conditions in hand, an array of postconsumer waste PS plastics was examined to validate the utility of this protocol. As shown in Figure 3, disposable PS spoons (**PS-2**) and cups (**PS-3**) commonly found in kitchens were compatible with this approach, yielding 2,4-diphenylthiophene with yields of 31% and 30%, respectively, and 1,3,5-triphenylbenzene with yields of 15% and 14%. Furthermore, PS components retrieved from discarded refrigerators (**PS-4**) also reacted with S_8 under concentrated sunlight to produce the target products (**1**, 29%; **2**, 14%). PS-based food packaging materials, including cake cups (**PS-5**), yogurt containers (**PS-6, 7**), instant noodle bowls (**PS-8**), and cup lids (**PS-9**), could all be upcycled into 2,4-diphenylthiophene (**1**, 18−28%) and 1,3,5-triphenylbenzene (**2**, 10−13%). Notably, materials with darker colors (**PS-6, 7, 8, and 9**) exhibited reduced yields of 2,4-diphenylthiophene and 1,3,5-triphenylbenzene, accompanied by an increase in styrene yield. This could be attributed to the fact that the dark additives in these materials acted as photothermal agents, whose photothermal effect under illumination made the pyrolysis of PS too fast, thereby decreasing target products formation. It was consistent with our observations from condition optimization experiments where an exogenous photothermal agent was added. Common PS-based laboratory items such as disposable test tubes (**PS-10**), sample vials (**PS-11**), foamed plastics (**PS-12**), and culture plates (**PS-13**) were also efficiently upcycled into products **1** (27−29%) and **2** (13−14%).

To further evaluate the substrate scope of this protocol, reactions of various polymers with elemental sulfur were investigated (Tables S11−S14). Poly(4-chlorostyrene), a polymer featuring an electron-withdrawing group on the phenyl ring, could be converted to 2,4-bis(4-chlorophenyl)-thiophene (**4**, 13%) and 1,3,5-tris(4-chlorophenyl)benzene (**5**, 7%). Similarly, poly(4-methylstyrene), a polymer bearing an electron-donating group on the phenyl ring, underwent reaction with S_8 to afford 2,4-di-*p*-tolylthiophene (**6**, 7%) and 1,3,5-tris(4-methylphenyl)benzene (**7**, 4%). These yields were lower than those achieved with PS, which presumably arose from the high reactivity of benzylic methyl groups toward sulfur radicals. Reaction of the binary styrene-acrylonitrile (SAN) copolymer (styrene/acrylonitrile = 1.7:1) with S_8 yielded four major products, including **1** (12%), **2** (5%), 5-phenylthiophene-3-carbonitrile (**8**, 10%), and *m,m*-diphenylbenzonitrile (**9**, 9%). The ternary acrylonitrile−butadiene−styrene (ABS) copolymer (styrene/butadiene/acrylonitrile = 3.1:1:2.3) produced a product profile comparable to that of SAN resin (**1**, 6%; **2**, 3%; **8**, 6%; **9**, 5%). Notably, no substituted thiophene or benzene derivatives were detected when styrene−butadiene−styrene (SBS) copolymer or poly(*α*-methylstyrene) (PAMS) were subjected to the identical reaction conditions. These results demonstrate that our method exhibits excellent compatibility with various PS wastes, even when they contain additives that typically impede recycling.

To investigate the reaction mechanism, a range of mechanistic experiments were conducted (Figure 4). Initially, to determine whether styrene detected in the reaction system acted as an intermediate, styrene was reacted with S_8 under irradiation. The reaction afforded 2,4-diphenylthiophene (**1**, 21%) and 2,5-diphenylthiophene (**10**, 12%), a product distribution entirely distinct from that observed when PS was employed as the substrate (Figure 4a). This result precludes styrene from serving as a reaction intermediate. In the absence of S_8, only trace amounts of 1,3,5-triphenylbenzene were obtained from PS in the presence of the photothermal agent (CB), highlighting sulfur's pivotal role in 1,3,5-triphenylbenzene formation (Figure 4b). When PS, poly(4-chlorostyrene), and S_8 were reacted together, only thiophenes and benzenes substituted with identical groups were produced (Figure 4c). This rules out the possibility that the products result from reactions between polymer molecular chains. In contrast, the reaction of an alternating copolymer of two distinct monomers with S_8 yielded only thiophenes and benzenes bearing alternating substituents (Figure 4d). The retention of this alternating arrangement of different substituents in products reveals that intramolecular aryl migration and rearrangement are not involved in the formation of target products.

To further explore the polymer chain changes, the reaction was monitored. Notably, a white LED was used as the light source to facilitate the control of the variables. After a series of condition optimizations, PS reacted with 0.2 equiv of S_8 under white LED irradiation to afford 2,4-diphenylthiophene (26% yield) and 1,3,5-triphenylbenzene (13% yield) in 6 min. First, gel permeation chromatography (GPC) analysis was performed on **dPS** collected at different reaction times (Figure 4e). The results showed that the molecular weight of PS remained essentially unchanged after 1 min of reaction, indicating that the polymer had not yet reacted. When the reaction proceeded to 2 min, a significant decrease in the molecular weight of the polymer was observed, suggesting partial cleavage of the polymer chains. At 3 min of reaction, a bimodal molecular weight distribution emerged. It is speculated that part of the polymer combines with sulfur, leading to an increase in molecular weight, while another part continues to undergo chain cleavage, resulting in a further decrease in molecular weight. The **dPS** isolated at this stage could generate small amounts of 2,4-diphenylthiophene (1%), 1,3,5-triphenylbenzene (2%), and styrene (4%) upon white

https://doi.org/10.1021/jacs.6c01318
J. Am. Chem. Soc. 2026, 148, 10193−10204

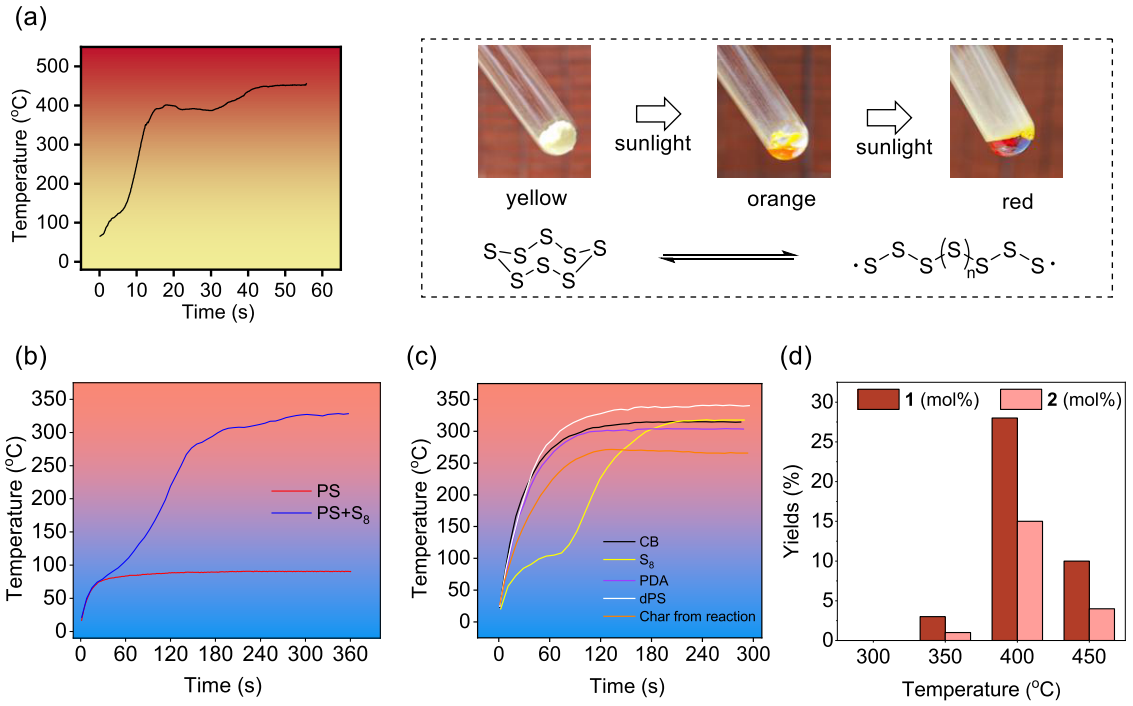

Figure 5. Photothermal effect investigation. (a) Temperature and state changes of elemental sulfur under sunlight irradiation. (b) Temperature measurement of reaction systems under white LED irradiation. (c) Temperature measurement for comparative study of different photothermal agents under white LED irradiation. (d) Product yields at different temperatures under bulk heating.

LED irradiation without additional S_8 (Table S15), which supports the plausibility of this hypothesis. After 4 min of reaction, the molecular weight reached a minimum and no longer changed. The **dPS** obtained after 6 min of reaction could hardly be converted into the target products (Table S15).

Subsequently, to gain more insight into the structural changes of the polymer, nuclear magnetic resonance (NMR) measurements were performed on the reaction systems at different reaction times. ^{1}H NMR spectra (Figure 4f) revealed that PS remained unchanged after 1 min of reaction, which is consistent with the GPC results. When the reaction proceeded for 2 min, most of the C(sp^3)-H disappeared and characteristic peaks of the product began to emerge. By 3 min of reaction, all of the C(sp^3)-H on the PS chains had completely vanished. Notably, the signal peak of hydrogen sulfide (H_2S) was detected at 2 min, and this finding is further confirmed by high-resolution mass spectrometry (HRMS) (Figure S45). Quantitative analysis of H_2S showed a yield of 58% relative to the amount of sulfur used. These results demonstrate that PS undergoes dehydrogenation with S_8 acting as the hydrogen acceptor. It is hypothesized that unsaturated carbon−carbon double bonds are formed after dehydrogenation. ^{13}C NMR spectra (Figure 4g) at 3 min of reaction exhibit distinct sp^2 carbon signals (excluding those of the product) in the range 135−145 ppm, which further validates this hypothesis. FT-IR spectroscopy (Figure 4h) results are consistent with the NMR data: no structural changes of PS were observed within 1 min, and C(sp^3)-H had completely disappeared by 3 min. Meanwhile, the product yields were monitored over time (Figure 4i). From 1 to 3 min, the yields increased slowly; after 3 min (when all C(sp^3)-H had vanished), the product yields rapidly rose to near their maximum value within 1 min. Collectively, these experimental results indicate that during the conversion of PS to the target products, chain scission and HAA occur first to generate sulfur-containing and unsaturated intermediates, which subsequently undergo further transformation to form the target product.

Notably, the ratio of yield of 2,4-diphenylthiophene to 1,3,5-triphenylbenzene (approximately 2:1) remained unchanged with the reaction time. Given that one product contains sulfur while the other is sulfur-free, the effect of sulfur dosage on product selectivity was first investigated (Figure 4j). Although the sulfur dosage significantly affected the product yield, it exerted a negligible influence on the ratio of the two products. Varying the distance between the reactor and the LED (adjusting the light intensity) also did not alter this ratio (Figure 4k). Since sulfur readily converts to free radicals under heating conditions, we hypothesize that the reaction proceeds via a free radical mechanism. Addition of the free radical scavengers BHT and DMPO to the reaction system significantly suppressed the formation of the target products (Figure 4l). Furthermore, EPR measurements of the reaction mixture after irradiation detected distinct carbon radical signals (Figure 4m). The sulfur radical signal may have been masked by the intense carbon radical signal, thus failing to be clearly observed. However, irradiation of elemental sulfur alone resulted in the detection of radicals (Figure S48).

During the EPR experiment, it was observed that S_8 underwent a notable temperature rise after irradiation. Furthermore, previous control experiments (Figure 2, entry 2) demonstrate that PS cannot be transformed in the absence of S_8, highlighting that the temperature elevation behavior of S_8 under irradiation is critical to PS conversion. To investigate this, 500 mg of S_8 in a tube was exposed to concentrated sunlight, with its temperature changes monitored by a thermocouple (Figure 5a). Yellow S_8 began to warm under illumination and gradually melted; as irradiation persisted, the

https://doi.org/10.1021/jacs.6c01318
J. Am. Chem. Soc. 2026, 148, 10193−10204

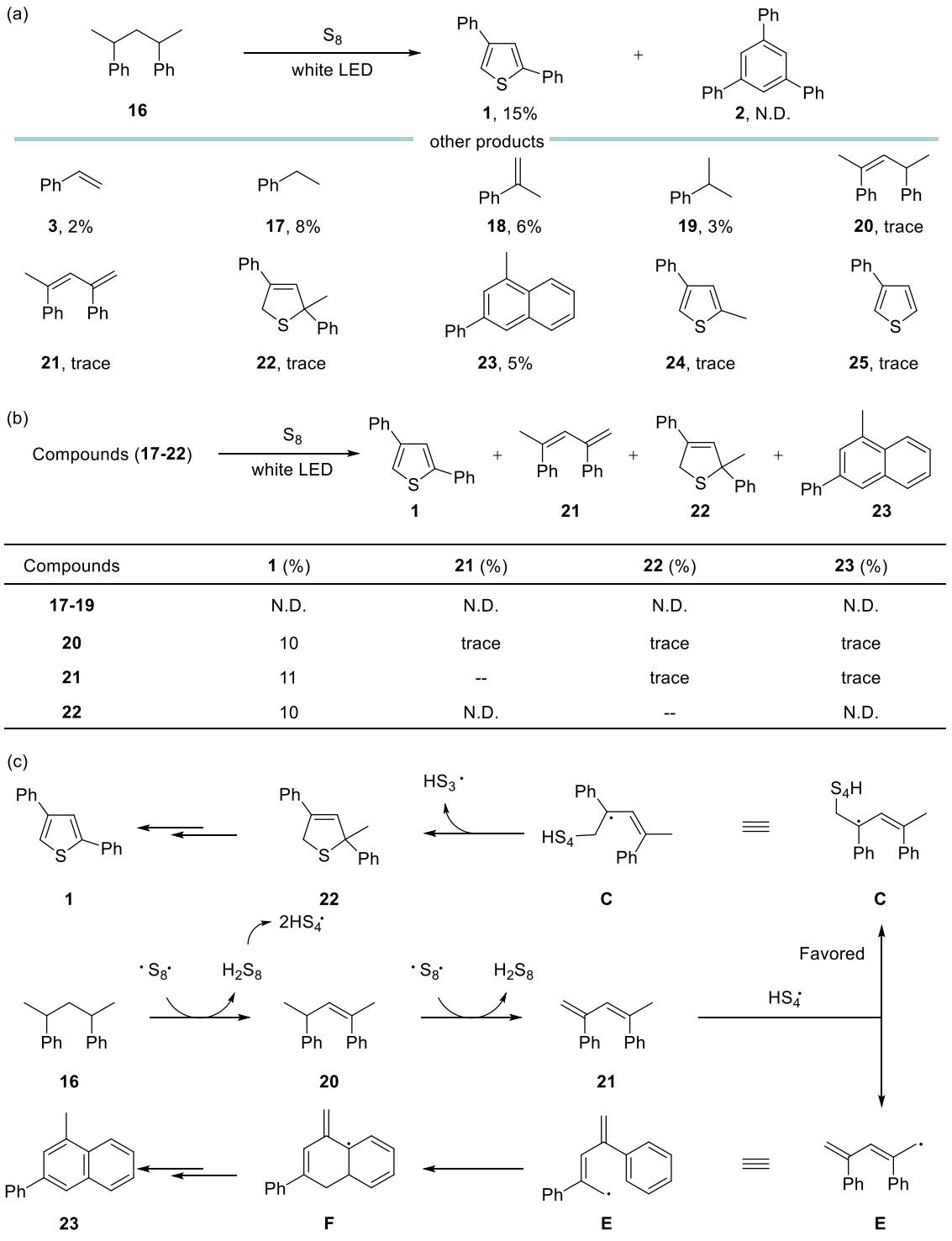

Compounds	**1** (%)	**21** (%)	**22** (%)	**23** (%)
17-19	N.D.	N.D.	N.D.	N.D.
20	10	trace	trace	trace
21	11	--	trace	trace
22	10	N.D.	--	N.D.

Figure 6. Mechanistic studies using dimeric PS model compound **16**. (a) Reaction of **16** with S_8 under white LED irradiation. (b) Validation of reaction intermediates. (c) Proposed mechanism.

system temperature rose continuously, and the molten sulfur turned orange, with the color intensifying, accompanied by an accelerated rate of temperature increase. This indicates that sulfur may exhibit enhanced light absorption capacity at elevated temperatures. This speculation was confirmed by ultraviolet−visible-near-infrared (UV−vis-NIR) spectroscopy of elemental sulfur, which showed a significant increase in visible light absorption under high-temperature conditions (Figure S52). When S_8 turned dark red, the temperature could reach 450 °C; with prolonged irradiation, black substances began to form in the system and the temperature rose further. This temperature-dependent color change of elemental sulfur is consistent with previous reports, which have thoroughly demonstrated that elemental sulfur undergoes ring opening at high temperatures, generating sulfur radicals.[11b]

Under irradiation with a white LED, the temperature of the reaction system was measured via thermal imaging (Figure 5b). The mixture of S_8 and PS could be rapidly heated to about 320

https://doi.org/10.1021/jacs.6c01318
J. Am. Chem. Soc. 2026, 148, 10193−10204

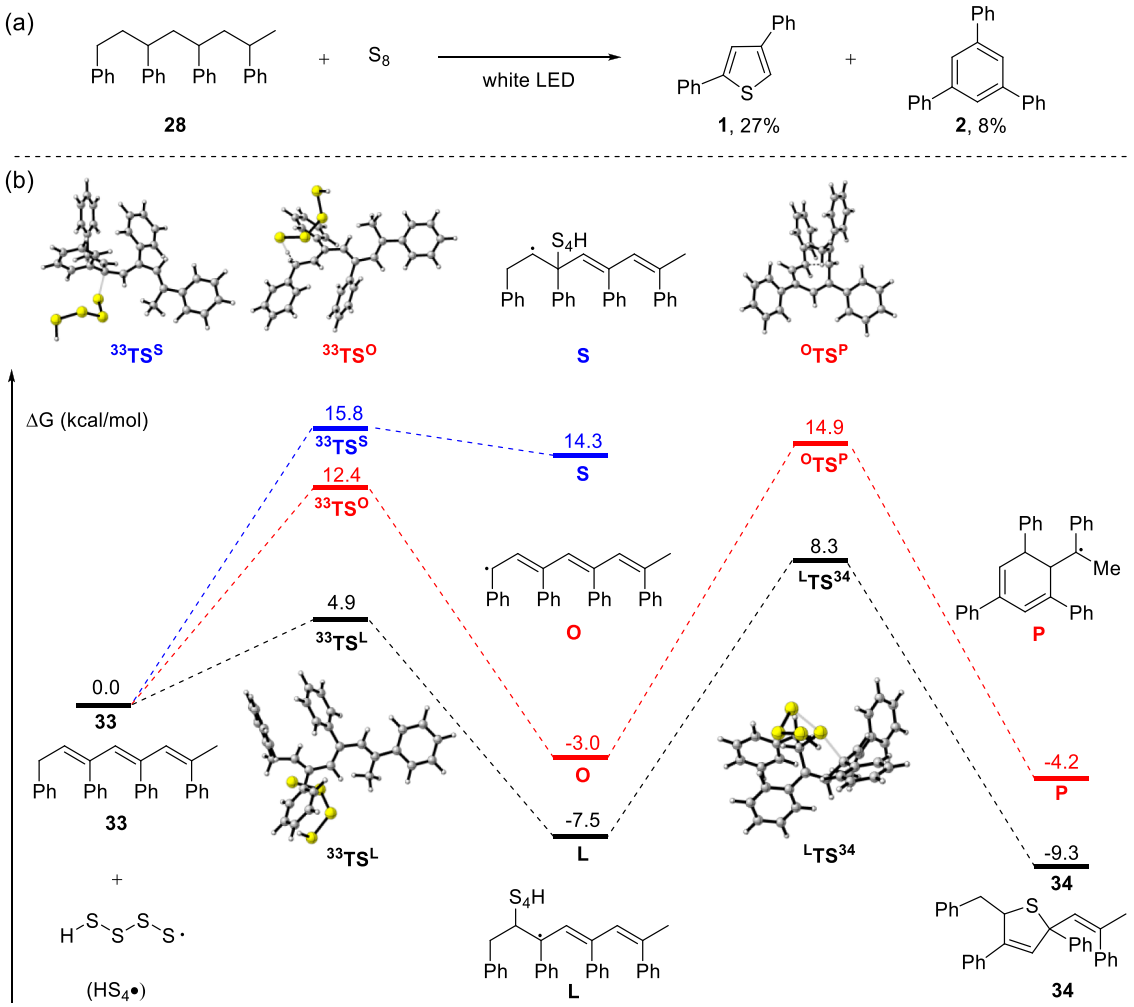

Figure 7. Computational data for the reaction of tetrameric PS model compound **28**. (a) Reaction of **28** with S_8 under white LED irradiation. (b) DFT calculations.

°C under irradiation, whereas in the absence of S_8, only a slight temperature increase of PS was observed. Integrating experimental observations with previous reports, we propose that sulfur acts not only as a reactant in the reaction but also as a photothermal agent, converting sunlight into thermal energy required for the reaction. Notably, after the reaction, the color of the reaction mixture deepened significantly and dark-colored **dPS** and char could be isolated therefrom. Both materials also exhibited prominent photothermal effects under light irradiation. When comparing S_8, **dPS**, char, and known photothermal agents (CB and polydopamine) under LED irradiation (Figure 5c), it was found that while S_8 exhibited a slower heating rate than CB and polydopamine (PDA), the maximum temperature it achieved was comparable to that of the latter two. In contrast, the char isolated from the reaction system showed a lower photothermal efficiency than CB and PDA. **dPS** displayed an initial heating rate similar to those of CB and PDA, and the maximum temperature it reached was slightly higher than that of the two known photothermal agents. Based on the above experimental results, it can be concluded that S_8 serves as the initial photothermal agent in the reaction to elevate the system temperature and initiate the reaction. After S_8 was consumed to form photothermally active **dPS** and char, these two products subsequently sustained the reaction temperature by continuing to convert light to thermal energy.

Bulk heating experiments showed that both excessively high and low temperatures were unfavorable for product formation, with yields under bulk heating conditions lower than those achieved under solar irradiation (Figure 5d). This phenomenon is likely attributed to the distinct temperature ranges required for different reaction stages. Utilizing S_8 as the initial photothermal agent enabled the reaction system temperature to align with the optimal window for intermediate generation and product formation. In contrast, the addition of extra photothermal agents may induce rapid temperature elevation and local overheating, leading to excessive scission of PS to form styrene and undesirable excessive dehydrogenative carbonization. The thermogravimetric (TG) curves (Figure S56) of the PS/S_8 mixture and pure PS further support this conclusion. Furthermore, the feasibility of the reaction between PS and S_8 under heating conditions enhances its operability, rendering it potentially compatible with large-scale existing photothermal equipment.[22]

To obtain more detailed mechanistic insights, mechanistic investigations were conducted using the dimeric PS model compound **16** (Figure 6a). Under white LED irradiation, compound **16** reacted with S_8 to produce 2,4-diphenylthiophene but failed to generate 1,3,5-triphenylbenzene. Besides the target product, a variety of side products (compounds **3**, **17**−**25**) were detected in the reaction system. These

https://doi.org/10.1021/jacs.6c01318
J. Am. Chem. Soc. 2026, 148, 10193−10204

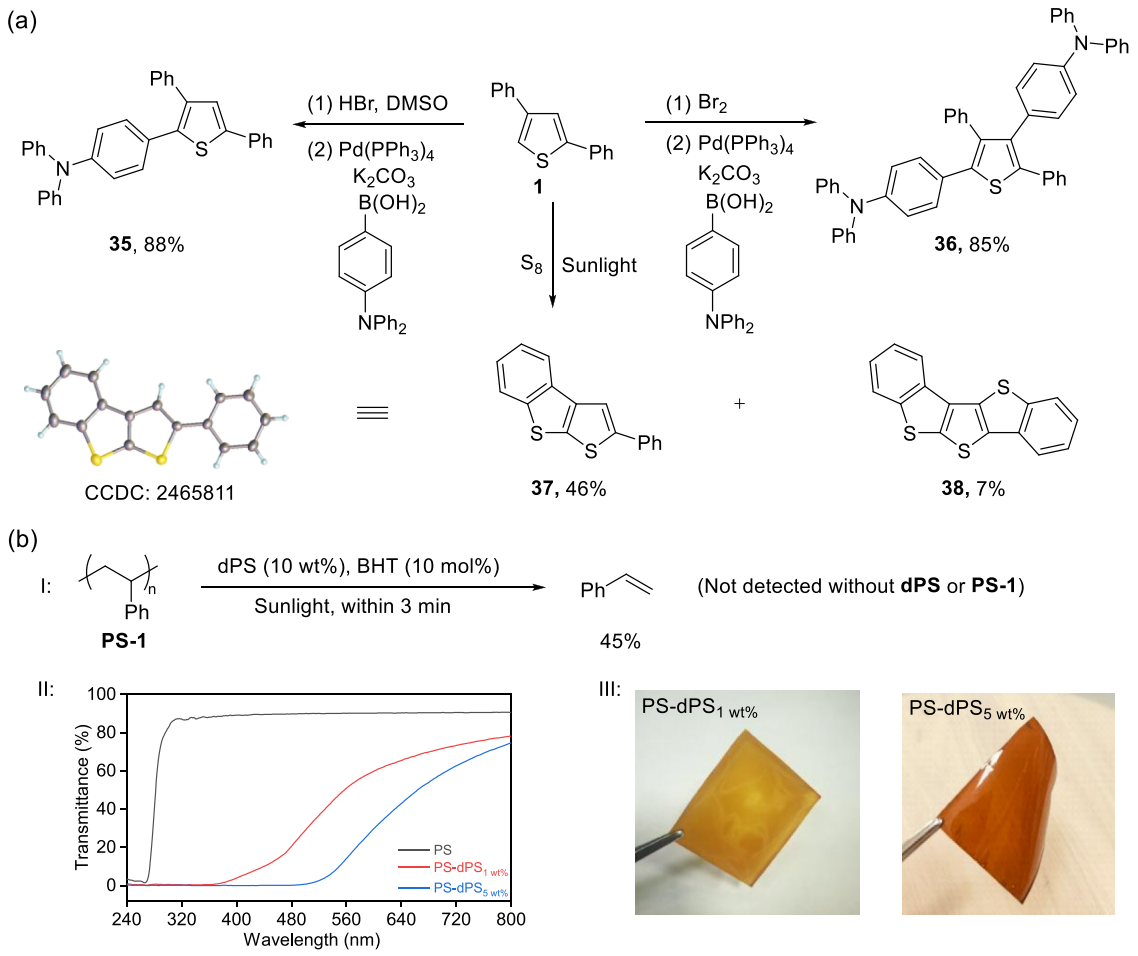

Figure 8. Product applications. (a) Transformation of 2,4-diphenylthiophene. (b) Applications of **dPS**. I: depolymerization of PS using **dPS** as the photothermal agent. II: UV−vis analysis. III: images of the PS film doped with **dPS**.

compounds were individually reacted with S_8 to verify their potential as reaction intermediates (Figure 6b). In previous experiments, the possibility of styrene (**3**) being an intermediate was already ruled out. Reactions of ethylbenzene (**17**), α-methylstyrene (**18**), and cumene (**19**) with S_8 did not yield the target product, indicating that they are not reaction intermediates either. When olefin **20** reacted with S_8 under irradiation, in addition to the thiophene product, diene **21**, tetrahydrothiophene compound **22**, and naphthalene compound **23** were also formed. **21** could also generate 2,4-diphenylthiophene as well as **22** and **23**, while **22** only yielded 2,4-diphenylthiophene. These experimental results demonstrate that compounds **20**, **21**, and **22** are probably all intermediates for thiophene formation: **21** is derived from **20**, and **22** is derived from **21**. In addition, **20** and **21** also serve as intermediates for the generation of side-product **23**.

Based on the above experiments, a reaction mechanism for the formation of 2,4-diphenylthiophene and side-product **23** is proposed as follows (Figure 6c). Upon irradiation, S_8 undergoes a temperature elevation and generates sulfur radicals. The dimeric PS model compound **16** reacts with sulfur radicals and occurs with dehydrogenation to form olefin **20**, which further reacts with sulfur radicals to produce diene **21** and polysulfane (H_2S_8). Notably, under heating conditions, polysulfane can not only generate H_2S but also produce various sulfur radical species.[23] To simplify the mechanism, only the homolytic cleavage of H_2S_8 to generate sulfur radical species $HS_4^{\bullet}$ is shown. There are two competing pathways for the reaction of sulfur radical $HS_4^{\bullet}$ with diene **21**. In the first pathway, it undergoes radical addition to form intermediate **C**, which subsequently generates intermediate **22** via intramolecular cyclization. Intermediate **22** then eliminates a methyl group to yield the target product **1** (more detailed mechanism see Figure S60). In the second pathway, HAA occurs to yield intermediate **E**, where the methyl radical in **E** can add to the unsaturated bond of the benzene ring, forming intermediate **F**. Then **F** undergoes dehydrogenation mediated by sulfur-centered radicals to yield side-product **23**. Density functional theory (DFT) calculations reveal that the radical addition pathway exhibits a lower energy barrier and intermediate **C** is more stable than intermediate **E**. Consequently, diene **21** preferentially forms intermediate **C**. This results in a higher yield of target product **1** compared to side-product **23**. Notably, the addition of the methyl radical in intermediate **E** to the benzene ring requires overcoming a high energy barrier due to the dearomatization of the benzene ring. If the alkyl chain is sufficiently long, the methyl radical would more readily undergo addition-cyclization with double bonds formed on the alkyl chain. This is presumably the pathway for the formation of 1,3,5-triphenylbenzene from PS. Product selectivity arises from the reaction between the sulfur radical and olefin, such that changes in external conditions did not affect the product ratio. This accounts for the constant ratio of

https://doi.org/10.1021/jacs.6c01318
J. Am. Chem. Soc. 2026, 148, 10193−10204

2,4-diphenylthiophene and 1,3,5-triphenylbenzene products generated from PS.

To validate the hypothesis, the tetrameric PS model compound **28** was reacted with S_8 under white LED light irradiation (Figure 7a). As expected, compound **28** yielded both 2,4-diphenylthiophene (27%) and 1,3,5-triphenylbenzene (8%). To gain more insight into the mechanism of the PS/S_8 reaction, a detailed computational study of the transformation was performed. Calculations reveal that following C=C bond formation via a HAA process, tetramer **28** readily undergoes further olefination to generate additional double bonds (Figure S68). Compound **33** is selected as a key intermediate to delineate the divergent pathways leading to 2,4-diphenylthiophene and 1,3,5-triphenylbenzene (Figure 7b). In the reaction of compound **33** with the sulfur radical ($HS_4^{\bullet}$), two distinct reactions are considered: radical addition or HAA. Two possible addition modes exist in the radical addition: one forms the secondary carbon-centered radical **S** with an energy barrier of 15.8 kcal mol^{-1} (^{33}**TS**^{S}) and the other generates the tertiary carbon-centered radical **L** with a lower barrier of 4.9 kcal mol^{-1} (^{33}**TS**^{L}). Given the higher energy barrier for **S** formation and its endergonic process, the radical addition reaction is significantly favored toward the formation of intermediate **L**. In contrast, HAA from an allylic C−H in **33** by $HS_4^{\bullet}$ exhibits an energy barrier of 12.4 kcal mol^{-1} (^{33}**TS**^{O}) in the formation of intermediate **O**. Notably, ^{33}**TS**^{O} exhibits a substantially higher energy barrier than ^{33}**TS**^{L}. Subsequent intramolecular cyclization of intermediate **L** via ^{L}**TS**^{34} (ΔG = 15.8 kcal mol^{-1}) yields intermediate **34** (the precursor to 2,4-diphenylthiophene), while intermediate **O** proceeds through transition state ^{O}**TS**^{P} (ΔG = 17.9 kcal mol^{-1}) to generate intermediate **P** (the precursor to 1,3,5-triphenylbenzene). These computational results rationalize the differences between the formation of 2,4-diphenylthiophene and 1,3,5-triphenylbenzene. Although **2** is thermodynamically more stable than **1**, the energy barrier for **1** formation is lower; consequently, at elevated temperatures, **1** was obtained in a higher yield. The selectivity toward the two products stems from the divergent reaction modes between $HS_4^{\bullet}$ and olefin **33**. Therefore, variations in certain reaction conditions, such as the dosage of elemental sulfur and light intensity, did not alter the product selectivity, resulting in a nearly constant product ratio. Based on the calculation results, a detailed reaction mechanism is proposed (Figure S61). Given the structural similarity between PS and the model compound, they are inferred to undergo analogous reaction pathways.

Gram-scale transformation of PS under sunlight has been successfully achieved, albeit with lower product yields (**1**, 21%; **2**, 10%) (see Section 10 of the Supporting Information for details). The products derived from the coupcycling of PS and S_8 all exhibit considerable application potential (Figure 8). 2,4-Diphenylthiophene, upon bromination and coupling reactions, yielded polysubstituted thiophenes **35** and **36** with 88% and 85% yields, respectively (Figure 8a). These two compounds share similar backbone structures with some optoelectronic materials, endowing them with promising potential applications.[24] 2,4-Diphenylthiophene and S_8 could react further under sunlight irradiation to form products benzo[*b*]thieno[3,2-*d*]thiophene **37** and dibenzo[*d*,*d*′]thieno[2,3-*b*;4,5-*b*′]-dithiophene **38**. The structure of **37** was unambiguously verified by X-ray single-crystal analysis (CCDC: 2465811), while **38** is a high-performance semiconductor material.[25] Another product, 1,3,5-triphenylbenzene, is a rigid planar aromatic molecule with C_3 symmetry, priced above $400 per kilogram. Its unique aromatic structure enables widespread use in synthesizing functional materials.[26] Given the pronounced photothermal effect of **dPS**, this material represents a promising candidate for photothermal applications. This capability is well exemplified by the successful depolymerization of PS using **dPS** as the photothermal agent (Figure 8b, part I). Furthermore, **dPS** could also function as an effective UV-blocking additive for PS plastics. Upon incorporation of **dPS** into PS to form a homogeneous film, the resultant material exhibited a significantly reduced UV transmittance relative to pure PS (Figure 8b, II and III). It should be noted that carbonyl moieties generated in **dPS** under ambient air conditions may shorten the service life of PS, yet their formation can be fully suppressed under oxygen-free environments. These experimental findings highlight that **dPS** also possesses substantial application prospects.

CONCLUSIONS

In conclusion, we have developed a solar-driven coupcycling strategy for PS and elemental sulfur. This strategy enables the rapid conversion of PS into 2,4-diphenylthiophene and 1,3,5-triphenylbenzene via the photothermal effect under solvent-free ambient air conditions. Successful conversion of various real-world waste PS plastics demonstrated the robust applicability of this approach. Mechanistic investigations demonstrate that elemental sulfur plays a dual role in the reaction, serving as both the initial photothermal agent and a reactant. The in situ-generated photothermal agents enable the maintenance of the reaction temperature. The use of well-defined dimeric and tetrameric PS model compounds permits direct characterization of reaction intermediates, thereby providing valuable insights into the reaction mechanism. Experimental and computational studies reveal that the reaction proceeds via a sulfur-radical-involved HAA process, yielding olefin intermediates. The selectivity toward the two products stems from the distinct reaction pathways of olefin intermediates with sulfur-containing radicals. This work has led to important fundamental outcomes relevant to the photothermal reactions of sulfur and the transformation of PS. It represents a simple and efficient method for the upcycling of waste plastics using clean energy.

ASSOCIATED CONTENT

Supporting Information

The Supporting Information is available free of charge at https://pubs.acs.org/doi/10.1021/jacs.6c01318.

Experimental details and characterization data (PDF)

Accession Codes

Deposition Number 2465811 contains the supplementary crystallographic data for this paper. These data can be obtained free of charge via the joint Cambridge Crystallographic Data Centre (CCDC) and Fachinformationszentrum Karlsruhe Access Structures service.

AUTHOR INFORMATION

Corresponding Authors

Heng Liu − *Dalian Institute of Chemical Physics, Chinese Academy of Sciences, Dalian 116023, China*;
Email: liuheng@dicp.ac.cn

https://doi.org/10.1021/jacs.6c01318
J. Am. Chem. Soc. 2026, 148, 10193−10204

Zhang-Pei Chen − *Center for Molecular Science and Engineering, College of Science, Northeastern University, Shenyang 110819, China;* orcid.org/0000-0002-0180-1462; Email: chenzhangpei@mail.neu.edu.cn

Jian-She Hu − *Center for Molecular Science and Engineering, College of Science, Northeastern University, Shenyang 110819, China;* orcid.org/0000-0003-0624-0788; Email: hujs@mail.neu.edu.cn

Qing-An Chen − *Dalian Institute of Chemical Physics, Chinese Academy of Sciences, Dalian 116023, China; University of Chinese Academy of Sciences, Beijing 100049, China;* orcid.org/0000-0002-9129-2656; Email: qachen@dicp.ac.cn

Authors

Yong Liu − *Center for Molecular Science and Engineering, College of Science, Northeastern University, Shenyang 110819, China; Dalian Institute of Chemical Physics, Chinese Academy of Sciences, Dalian 116023, China*

Zhi-Hui Wang − *Dalian Institute of Chemical Physics, Chinese Academy of Sciences, Dalian 116023, China; University of Chinese Academy of Sciences, Beijing 100049, China*

Yilitabaier Julaiti − *Dalian Institute of Chemical Physics, Chinese Academy of Sciences, Dalian 116023, China; University of Chinese Academy of Sciences, Beijing 100049, China*

Complete contact information is available at: https://pubs.acs.org/10.1021/jacs.6c01318

Notes

The authors declare no competing financial interest.

■ ACKNOWLEDGMENTS

Financial support from the National Natural Science Foundation of China (22402191) and Dalian Science and Technology Talent Innovation Support Policy Project (2024RQ088) is acknowledged.

■ REFERENCES

(1) Geyer, R.; Jambeck, J. R.; Law, K. L. Production, Use, and Fate of all Plastics Ever Made. *Sci. Adv.* **2017**, *3*, No. e1700782.

(2) (a) Ellis, L. D.; Rorrer, N. A.; Sullivan, K. P.; Otto, M.; McGeehan, J. E.; Román-Leshkov, Y.; Wierckx, N.; Beckham, G. T. Chemical and Biological Catalysis for Plastics Recycling and Upcycling. *Nat. Catal.* **2021**, *4*, 539−556. OECD. Global Plastics Outlook: Economic Drivers, *Environmental Impacts and Policy Options*; OECD Publishing, 2022..

(3) (a) Rahimi, A.; García, J. M. Chemical Recycling of Waste Plastics for New Materials Production. *Nat. Rev. Chem.* **2017**, *1*, 0046. (b) Chamas, A.; Moon, H.; Zheng, J.; Qiu, Y.; Tabassum, T.; Jang, J. H.; Abu-Omar, M.; Scott, S. L.; Suh, S. Degradation Rates of Plastics in the Environment. *ACS Sustain. Chem. Eng.* **2020**, *8*, 3494−3511. (c) Stubbins, A.; Law, K. L.; Muñoz, S. E.; Bianchi, T. S.; Zhu, L. Plastics in the Earth System. *Science* **2021**, *373*, 51−55. (d) Xu, Z.; Sun, D.; Xu, J.; Yang, R.; Russell, J. D.; Liu, G. Progress and Challenges in Polystyrene Recycling and Upcycling. *ChemSusChem* **2024**, *17*, No. e202400474.

(4) (a) Luo, X.; Wei, Z.; Seo, B.; Hu, Q.; Wang, X.; Romo, J. A.; Jain, M.; Cakmak, M.; Boudouris, B. W.; Zhao, K.; et al. Circularly Recyclable Polymers Featuring Topochemically Weakened Carbon−Carbon Bonds. *J. Am. Chem. Soc.* **2022**, *144*, 16588−16597. (b) He, S-F.; Xu, T.; Wan, Q.; Tang, K.; Chen, X.; Li, D.; Jiang, Y.; Zhai, C.; Zhu, C.; Shen, T. Divergent Upcycling of Polystyrene into Phenol and Hydroquinone Derivatives by Photocatalysis and Electrocatalysis. *Angew. Chem., Int. Ed.* **2025**, *64*, No. e202508166.

(5) (a) Yeung, C. W. S.; Teo, J. Y. Q.; Loh, X. J.; Lim, J. Y. C. Polyolefins and Polystyrene as Chemical Resources for a Sustainable Future: Challenges, Advances, and Prospects. *ACS Mater. Lett.* **2021**, *3*, 1660−1676. (b) Peng, Y.; Wang, Y.; Ke, L.; Dai, L.; Wu, Q.; Cobb, K.; Zeng, Y.; Zou, R.; Liu, Y.; Ruan, R. A Review on Catalytic Pyrolysis of Plastic Wastes to High-Value Products. *Energy Convers. Manage.* **2022**, *254*, 115243. (c) Cao, R.; Zhang, M.-Q.; Hu, C.; Xiao, D.; Wang, M.; Ma, D. Catalytic Oxidation of Polystyrene to Aromatic Oxygenates over a Graphitic Carbon Nitride Catalyst. *Nat. Commun.* **2022**, *13*, 4809. (d) Musa, A.; Jaseer, E. A.; Barman, S.; Garcia, N. Review on Catalytic Depolymerization of Polyolefin Waste by Hydrogenolysis: State-of-the-Art and Outlook. *Energy Fuels* **2024**, *38*, 1676−1691.

(6) (a) Wang, M.; Wen, J.; Huang, Y.; Hu, P. Selective Degradation of Styrene-Related Plastics Catalyzed by Iron under Visible Light. *ChemSusChem* **2021**, *14*, 5049−5056. (b) Zhang, G.; Zhang, Z.; Zeng, R. Photoinduced $FeCl_3$-Catalyzed Alkyl Aromatics Oxidation toward Degradation of Polystyrene at Room Temperature. *Chin. J. Chem.* **2021**, *39*, 3225−3230. (c) Huang, Z.; Shanmugam, M.; Liu, Z.; Brookfield, A.; Bennett, E. L.; Guan, R.; Vega Herrera, D. E.; Lopez-Sanchez, J. A.; Slater, A. G.; McInnes, E. J. L.; et al. Chemical Recycling of Polystyrene to Valuable Chemicals via Selective Acid-Catalyzed Aerobic Oxidation Under Visible Light. *J. Am. Chem. Soc.* **2022**, *144*, 6532−6542. (d) Li, T.; Vijeta, A.; Casadevall, C.; Gentleman, A. S.; Euser, T.; Reisner, E. Bridging Plastic Recycling and Organic Catalysis: Photocatalytic Deconstruction of Polystyrene via a C−H Oxidation Pathway. *ACS Catal.* **2022**, *12*, 8155−8163. (e) Qin, Y.; Zhang, T.; Ching, H. Y. V.; Raman, G. S.; Das, S. Integrated Strategy for the Synthesis of Aromatic Building Blocks via Upcycling of Real-Life Plastic Wastes. *Chem* **2022**, *8*, 2472−2484. (f) Sullivan, K. P.; Werner, A. Z.; Ramirez, K. J.; Ellis, L. D.; Bussard, J. R.; Black, B. A.; Brandner, D. G.; Bratti, F.; Buss, B. L.; Dong, X.; et al. Mixed Plastics Waste Valorization Through Tandem Chemical Oxidation and Biological Funneling. *Science* **2022**, *378*, 207−211. (g) Li, C.; Kong, X. Y.; Lyu, M.; Tay, X. T.; Đokić, M.; Chin, K. F.; Yang, C. T.; Lee, E. K. X.; Zhang, J.; Tham, C. Y.; et al. Upcycling of Non-Biodegradable Plastics by Base Metal Photocatalysis. *Chem* **2023**, *9*, 2683−2700. (h) Meng, J.; Zhou, Y.; Li, D.; Jiang, X. Degradation of Plastic Wastes to Commercial Chemicals and Monomers Under Visible Light. *Sci. Bull.* **2023**, *68*, 1522−1530. (i) Ong, A.; Teo, J. Y. Q.; Feng, Z.; Tan, T. T. Y.; Lim, J. Y. C. Organocatalytic Aerobic Oxidative Degradation of Polystyrene to Aromatic Acids. *ACS Sustain. Chem. Eng.* **2023**, *11*, 12514−12522. (j) Peng, Z.; Chen, R.; Li, H. Heterogeneous Photocatalytic Oxidative Cleavage of Polystyrene to Aromatics at Room Temperature. *ACS Sustain. Chem. Eng.* **2023**, *11*, 10688−10697. (k) Hourtoule, M.; Trienes, S.; Ackermann, L. Anodic Commodity Polymer Recycling: The Merger of Iron-Electrocatalysis with Scalable Hydrogen Evolution Reaction. *Angew. Chem., Int. Ed.* **2024**, *63*, No. e202412689. (l) Xu, S.; Liu, S.; Song, W.; Zheng, N. Metal-free Upcycling of Plastic Waste: Photo-Induced Oxidative Degradation of Polystyrene in Air. *Green Chem.* **2024**, *26*, 1363−1369. (m) Zhao, B.; Tan, H.; Yang, J.; Zhang, X.; Yu, Z.; Sun, H.; Wei, J.; Zhao, X.; Zhang, Y.; Chen, L.; et al. Catalytic Conversion of Mixed Polyolefins under Mild Atmospheric Pressure. *Innovation* **2024**, *5*, 100586. (n) Yu, Y.; Zhu, Y.; Liu, J.; Zhang, M.; Li, J.; Zhang, S.; Mei, Q. Highly Selective Aerobic Oxidation of Polystyrene to Benzoic Acid Catalyzed by Nitrogen Dioxide. *Sci. Bull.* **2025**, *70*, 2463−2472.

(7) Oh, S.; Stache, E. E. Chemical Upcycling of Commercial Polystyrene via Catalyst-Controlled Photooxidation. *J. Am. Chem. Soc.* **2022**, *144*, 5745−5749.

(8) (a) Yan, B.; Shi, C.; Beckham, G. T.; Chen, E. Y. X.; Román-Leshkov, Y. Electrochemical Activation of C−C Bonds through Mediated Hydrogen Atom Transfer Reactions. *ChemSusChem* **2022**, *15*, No. e202102317. (b) Oh, S.; Stache, E. E. Mechanistic Insights Enable Divergent Product Selectivity in Catalyst-Controlled Photo-oxidative Degradation of Polystyrene. *ACS Catal.* **2023**, *13*, 10968−10975.

(9) (a) Zhao, B.; Hu, Z.; Sun, Y.; Hajiayi, R.; Wang, T.; Jiao, N. Selective Upcycling of Polyolefins into High-Value Nitrogenated Chemicals. *J. Am. Chem. Soc.* **2024**, *146*, 28605−28611. (b) Zeng, G.; Su, Y.; Jiang, J.; Huang, Z. Nitrogenative Degradation of Polystyrene Waste. *J. Am. Chem. Soc.* **2025**, *147*, 2737−2746.
(10) Baek, D.; Al Abdulghani, A. J.; Walsh, D. J.; Hofsommer, D. T.; Gerken, J. B.; Shi, C.; Chen, E. Y. X.; Hermans, I.; Stahl, S. S. Can the Hock Process Be Used to Produce Phenol from Polystyrene? *J. Am. Chem. Soc.* **2025**, *147*, 8687−8694.
(11) (a) Lim, J.; Pyun, J.; Char, K. Recent Approaches for the Direct Use of Elemental Sulfur in the Synthesis and Processing of Advanced Materials. *Angew. Chem., Int. Ed.* **2015**, *54*, 3249−3258. (b) Boyd, D. A. Sulfur and Its Role in Modern Materials Science. *Angew. Chem., Int. Ed.* **2016**, *55*, 15486−15502.
(12) Jia, J.; Liu, J.; Wang, Z.-Q.; Liu, T.; Yan, P.; Gong, X.-Q.; Zhao, C.; Chen, L.; Miao, C.; Zhao, W.; et al. Photoinduced Inverse Vulcanization. *Nat. Chem.* **2022**, *14*, 1249−1257.
(13) Song, H.; Meng, J.; Jiang, X. Sulfur-Containing Sustainable Polymers: Synthetic Pathways, Degradation Mechanisms, and Multifunctional Applications. *Natl. Sci. Rev.* **2025**, *12*, nwaf475.
(14) Chung, W. J.; Griebel, J. J.; Kim, E. T.; Yoon, H.; Simmonds, A. G.; Ji, H. J.; Dirlam, P. T.; Glass, R. S.; Wie, J. J.; Nguyen, N. A.; et al. The Use of Elemental Sulfur as an Alternative Feedstock for Polymeric Materials. *Nat. Chem.* **2013**, *5*, 518−524.
(15) Meyer, B. Elemental sulfur. *Chem. Rev.* **1976**, *76*, 367−388.
(16) (a) Mayer, R. Elemental Sulfur and its Reactions. In *Organic Chemistry of Sulfur*; Oae, S., Ed.; Springer US, 1977; pp 33−69. (b) Nguyen, T. B. Recent Advances in Organic Reactions Involving Elemental Sulfur. *Adv. Synth. Catal.* **2017**, *359*, 1066−1130. (c) Bai, L.; Jiang, X. Smelless/Stable/Sustainable Sulfur Chemistry. *CCS Chem.* **2025**, *7*, 1889−1902.
(17) (a) Tang, Y.; Cen, Z.; Ma, Q.; Zheng, B.; Cai, Z.; Liu, S.; Wu, D. A Versatile Sulfur-Assisted Pyrolysis Strategy for High-Atom-Economy Upcycling of Waste Plastics into High-Value Carbon Materials. *Adv. Sci.* **2023**, *10*, 2206924. (b) Zhao, J.; Shu, Y.; Niu, Q.; Zhang, P. Processing Plastic Wastes into Value-Added Carbon Adsorbents by Sulfur-Based Solvothermal Synthesis. *ACS Sustain. Chem. Eng.* **2023**, *11*, 11207−11218.
(18) (a) Zhang, C.; Kang, Q.; Chu, M.; He, L.; Chen, J. Solar-Driven Catalytic Plastic Upcycling. *Trends Chem.* **2022**, *4*, 822−834. (b) Cao, R.; Xiao, D.; Wang, M.; Gao, Y.; Ma, D. Solar-driven Photocatalysis for Recycling and Upcycling Plastics. *Appl. Catal. B Environ.* **2024**, *341*, 123357. (c) Wimberger, L.; Ng, G.; Boyer, C. Light-Driven Polymer Recycling to Monomers and Small Molecules. *Nat. Commun.* **2024**, *15*, 2510. (d) Mountanea, O. G.; Skolia, E.; Kokotos, C. G. Photochemical Upcycling and Recycling of Plastics: Achievements and Future Opportunities. *Green Chem.* **2024**, *26*, 8528−8549.
(19) (a) Huang, R.; Zhao, Y.; Li, C.; Li, D.; Jiang, X. Photocatalytic Upcycling of Polysulfones at Ambient Conditions. *Nat. Sustain.* **2025**, *8*, 818−826. (b) Gu, B.; Li, C.; Jiang, X. Chemical Upcycling of Polyphenylene Sulfide at Room Temperature. *Adv. Sci.* **2025**, No. e19090.
(20) (a) Jiang, H.; Medina, E. A.; Stache, E. E. Upcycling Poly(vinyl chloride) and Polystyrene Plastics Using Photothermal Conversion. *J. Am. Chem. Soc.* **2025**, *147*, 2822−2828. (b) Kugelmass, L. H.; Tagnon, C.; Stache, E. E. Photothermal Mediated Chemical Recycling to Monomers via Carbon Quantum Dots. *J. Am. Chem. Soc.* **2023**, *145*, 16090−16097. (c) Oh, S.; Jiang, H.; Kugelmass, L. H.; Stache, E. E. Recycling of Post-Consumer Waste Polystyrene Using Commercial Plastic Additives. *ACS Cent. Sci.* **2025**, *11*, 57−65. (d) Xing, C.; Mao, C.; Wang, S.; Zhou, Y.; Wu, L.; Zhang, D.; Kang, D.; Yang, D.; Gong, W.; Wei, W.; et al. Ambient Solar Thermal Catalysis for Polyolefin Upcycling Using Copper Encapsulated in Silicon Nanosheets and Chloroaluminate Ionic Liquid. *Nat. Catal.* **2025**, *8*, 556−568. (e) Liu, Y.; Zhong, Q.; Xu, P.; Huang, H.; Yang, F.; Cao, M.; He, L.; Zhang, Q.; Chen, J. Solar Thermal Catalysis for Sustainable and Eefficient Polyester Upcycling. *Matter* **2022**, *5*, 1305−1317. (f) Lou, X.; Yan, P.; Jiao, B.; Li, Q.; Xu, P.; Wang, L.; Zhang, L.; Cao, M.; Wang, G.; Chen, Z.; et al. Grave-to-cradle Photothermal Upcycling of Waste Polyesters over Spent $LiCoO_2$. *Nat. Commun.* **2024**, *15*, 2730.
(21) Zhang, Z.; Hirose, T.; Nishio, S.; Morioka, Y.; Azuma, N.; Ueno, A.; Ohkita, H.; Okada, M. Chemical Recycling of Waste Polystyrene into Styrene over Solid Acids and Bases. *Ind. Eng. Chem. Res.* **1995**, *34*, 4514−4519.
(22) Koepf, E.; Alxneit, I.; Wieckert, C.; Meier, A. A Review of High Temperature Solar Driven Reactor Technology: 25 Years of Experience in Research and Ddevelopment at the Paul Scherrer Institute. *Appl. Energy* **2017**, *188*, 620−651.
(23) (a) Muller, E. F.; Hyne, J. B. Thermal Decomposition of Tri- and Tetrasulfanes. *J. Am. Chem. Soc.* **1969**, *91*, 1907−1912. (b) Bao, J.; Martin, K. P.; Cho, E.; Kang, K.-S.; Glass, R. S.; Coropceanu, V.; Bredas, J.-L.; Parker, W. O. N., Jr.; Njardarson, J. T.; Pyun, J. On the Mechanism of the Inverse Vulcanization of Elemental Sulfur: Structural Characterization of Poly(sulfur-random-(1,3-diisopropenylbenzene)). *J. Am. Chem. Soc.* **2023**, *145*, 12386−12397.
(24) Tanaka, E.; Nishizawa, T.; Yamada, Y.; Itoh, H.; Yamaguchi, A.; Nakatsuka, M. Tetraphenylthiophene Derivative and Electrophotographic Photoreceptor Containing Same, EP 317233 A2, 1989..
(25) Li, J.; Wang, P.; Dong, J.; Xie, Z.; Tan, X.; Zhou, L.; Ai, L.; Li, B.; Wang, Y.; Dong, H. A Domino Protocol toward High-Performance Unsymmetrical Dibenzo[*d*,*d*′]thieno[2,3-*b*;4,5-*b*′]-dithiophenes Semiconductors. *Angew. Chem., Int. Ed.* **2024**, *63*, No. e202400803.
(26) (a) Rommens, J.; Vaes, A.; Van der Auweraer, M.; De Schryver, F. C.; Bässler, H.; Vestweber, H.; Pommerehne, J. Dual Electroluminescence of an Amino Substituted 1,3,5-Triphenylbenzene. *J. Appl. Phys.* **1998**, *84*, 4487−4494. (b) Ribeiro da Silva, M. A. V.; Santos, L. M. N. B. F.; Lima, L. M. S. S. Thermodynamic Study of 1,2,3-Triphenylbenzene and 1,3,5-Triphenylbenzene. *J. Chem. Thermodyn.* **2010**, *42*, 134−139. (c) Subramaniyan@Raja, R.; Anandha Babu, G.; Ramasamy, P. Studies on the Growth and Characterization of an Organic Single Crystal − 1,3,5- Triphenylbenzene. *Mater. Res. Innovations* **2018**, *22*, 1−6. (d) Vishnoi, P.; Kaleeswaran, D.; Murugavel, R. 1,3,5-Triphenylbenzene: a Versatile Photoluminescent Chemo-sensor Platform and Supramolecular Building Block. *RSC Adv.* **2018**, *8*, 17535−17550. (e) Zhang, W.; Chen, L.; Niu, R.; Ma, Z.; Ba, K.; Xie, T.; Chu, X.; Wu, S.; Wang, D.; Liu, G. Transient-State Self-Bipolarized Organic Frameworks of Single Aromatic Units for Natural Sunlight-Driven Photosynthesis of H_2O_2. *Adv. Sci.* **2024**, *11*, 2308322. (f) Kaliramna, S.; Aryan; Dhayal, S. S.; Kumar, N. Optical and Electrical Properties of 1,3,5-Triphenylbenzene (TPB) Thin Film for Optoelectronic Devices. *Opt. Mater.* **2024**, *149*, 115087.

https://doi.org/10.1021/jacs.6c01318
J. Am. Chem. Soc. 2026, 148, 10193−10204